

Application of quaternions in error analysis of flexible CMMs

Q.J. Tang^{1,2,3}, Q. Yang^{3,*}, X.J. Wang², C.Y. Liu^{3,4}, C.Y. Ma²

¹*Key Laboratory of Optoelectronic Devices and Systems of Ministry of Education and Guangdong Province, College of Optoelectronic Engineering, Shenzhen University, Shenzhen 518060, China*

²*MOEMS Education Ministry Key Laboratory, Tianjin University, Tianjin 300072, P. R. China*

³*College of Engineering, Design and Physical Science, Brunel University London, UB8 3PH, UK*

⁴*Metrology and Calibration Unit, First Crust Deformation Monitoring and Application Center, CEA, Tianjin 300180, China*

Abstract

Flexible coordinate measuring machine (CMM) is a type of CMM with rotational joints and flexible arms, where linear measurements are replaced by angular measurements. Due to its large measuring range, small size and low weight, it has been widely used in many applications. Denavit-Hartenberg parametric method is often employed to describe the measuring equations and error models of flexible CMMs. On the other hand, it is well known the quaternions can be used to speed up calculations involving rotations. A quaternion is represented by just four scalars, compared with a 3×3 rotation matrix which has nine scalar entries. Since invented by W.R. Hamilton, quaternions have found applications in situations involving rotations. In this paper, we will present the detailed error analysis of flexible CMMs by means of quaternions and discuss the results in comparison with rotational matrix approaches.

1 Introduction

Flexible coordinate measuring machine (CMM) is a type of CMM with rotational joints and flexible arms, where linear measurements are replaced by

angular measurements. Due to its large measuring range, small size and low weight, it has been widely used in many applications [1].

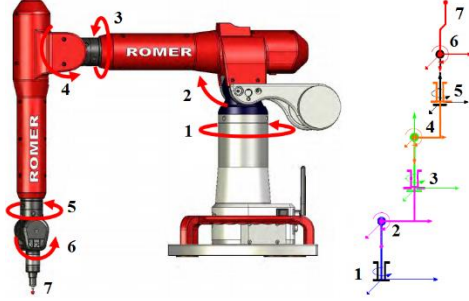


Figure 1: Flexible CMM and geometric diagram

As shown in Figure 1, the flexible CMM has six rotational arms, of which the two adjacent arms are perpendicular to each other at zero positions. The right figure is its geometric diagram with six coordinate systems. In 1955, Denavit and Hartenberg proposed a method, which used a homogeneous transformation matrix to describe the relationship between two different coordinate system [2-4].

$$T = \begin{bmatrix} n_x & o_x & a_x & p_x \\ n_y & o_y & a_y & p_y \\ n_z & o_z & a_z & p_z \\ 0 & 0 & 0 & 0 \end{bmatrix} \quad (1)$$

As shown in (1), it is often used to describe the transformation matrix from i th coordinate system to $(i - 1)$ th coordinate system, where (p_x, p_y, p_z) denotes the coordinates of the origin of i th system in the $(i - 1)$ th coordinate system. (n_x, n_y, n_z) , (o_x, o_y, o_z) and (a_x, a_y, a_z) denote direction cosines of x, y, z axes of i th system relative to $(i - 1)$ th coordinate system, respectively. Define $T_{(i-1)i}$ ($i = 1, 2, \dots, 6$) as the homogeneous transformation matrix from coordinate system i to system $(i - 1)$ in Figure 1. Then the measurement model can be obtained by the following transformation matrix:

$$T_{16} = T_{12}T_{23}T_{34}T_{45}T_{56} \quad (2)$$

The measurement model involves several matrix multiplications. When considering various errors, relevant matrices need to be expanded, which may introduce approximation (thus additional modelling error) and complexity. In this paper, we will employ quaternions to perform the modelling and error analysis of the flexible CMM.

2 Quaternions

2.1 Notations and definitions

Quaternions are invented by W.R. Hamilton, they can be used to speed up calculations involving rotations. As a quaternion is represented by just four scalars, in contrast to a 3×3 rotation matrix which has nine scalar entries [5].

A quaternion is defined as follows [6]:

$$Q = a\mathbf{i} + b\mathbf{j} + c\mathbf{k} + q_0 \quad (3)$$

where a, b, c, q_0 are real numbers, and $\mathbf{i}, \mathbf{j}, \mathbf{k}$ are the imaginary units which obey the following multiplication rules:

$$\begin{cases} \mathbf{i}^2 = \mathbf{j}^2 = \mathbf{k}^2 = -1 \\ \mathbf{ij} = -\mathbf{ji} = \mathbf{k} \\ \mathbf{ki} = -\mathbf{ik} = \mathbf{j} \\ \mathbf{jk} = -\mathbf{kj} = \mathbf{i} \end{cases} \quad (4)$$

Let $\mathbf{q} = a\mathbf{i} + b\mathbf{j} + c\mathbf{k}$, the equation (3) can be rewritten as:

$$Q = q_0 + \mathbf{q} \quad (5)$$

where q_0 denotes the scalar part, and \mathbf{q} denotes the vector part.

Given another quaternion $P(P = p_0 + \mathbf{p})$, their product according to the algebraic rules of multiplications given above is [6]:

$$PQ = (p_0 + \mathbf{p})(q_0 + \mathbf{q}) = p_0q_0 - \mathbf{p} \cdot \mathbf{q} + p_0\mathbf{q} + q_0\mathbf{p} + \mathbf{p} \times \mathbf{q} \quad (6)$$

where $\mathbf{p} \cdot \mathbf{q}$ and $\mathbf{p} \times \mathbf{q}$ represent the standard inner and cross products.

Meanwhile, $(p_0q_0 - \mathbf{p} \cdot \mathbf{q})$ is the product's scalar part, and $(p_0\mathbf{q} + q_0\mathbf{p} + \mathbf{p} \times \mathbf{q})$ denotes the vector part. If $p_0 = 0$ and $q_0 = 0$, $P = \mathbf{p}$, $Q = \mathbf{q}$ are pure quaternions and the product can then be simplified as:

$$PQ = -\mathbf{p} \cdot \mathbf{q} + \mathbf{p} \times \mathbf{q} \quad (7)$$

The norm of the quaternion Q is defined in (8):

$$\|Q\| = \sqrt{q_0^2 + |\mathbf{q}|^2} = \sqrt{q_0^2 + a^2 + b^2 + c^2} \quad (8)$$

If the norm is 1, the quaternion is called a unit quaternion.

The quaternion $Q^* = q_0 - \mathbf{q}$ is called the conjugate of Q , with the following properties:

$$Q^*Q = QQ^* = \|Q\|^2 \quad (9)$$

$$(PQ)^* = Q^*P^* \quad (10)$$

$$\|PQ\| = \|P\|\|Q\| \quad (11)$$

Given an arbitrary quaternion Q , it can be described as [7]:

$$Q = \|Q\|(\cos \alpha + \mathbf{n} \sin \alpha) \quad (12)$$

where \mathbf{n} is the unit quaternion, and $\mathbf{n} = \mathbf{q}/\|\mathbf{q}\|$, $\cos \alpha = q_0/\|Q\|$, $0 \leq \alpha < \pi$.

2.2 Quaternions and rotations

Let S be an arbitrary inertial reference frame with basic vectors being identified with $\mathbf{i}, \mathbf{j}, \mathbf{k}$ and \mathbf{r} be a given arbitrary vector, $R_s = r_0 + \mathbf{r}$. The unit quaternion Q presented in (13) can denote a counter-clockwise rotation which rotates an angle of 2α along the vector \mathbf{n} in the coordinate system S [7].

$$Q = \cos \alpha + \mathbf{n} \sin \alpha \quad (13)$$

When the given vector rotates an angle of 2α along the vector \mathbf{n} in the coordinate system S , the resulting vector R_s' can be computed through rotation transformation as:

$$R_s' = QR_sQ^* \quad (14)$$

where the vector part of R_s' is the rotated vector in the coordinate system.

If the vector \mathbf{r} goes through several rotations in the same inertial reference frame, the rotation quaternions are described as Q_1, Q_2, \dots, Q_k , and the resulting vector is :

$$R_s' = Q_k(\dots(Q_2(Q_1R_sQ_1^*)Q_2^*)\dots)Q_k^* \quad (15)$$

According to (10), equation (15) can be rewritten as follows:

$$R_s' = Q_k \dots Q_2 Q_1 R_s Q_1^* Q_2^* \dots Q_k^* = (Q_k \dots Q_2 Q_1) R_s (Q_k \dots Q_2 Q_1)^* \quad (16)$$

3 Measurement model and error analysis

3.1 Measurement model based on quaternions

In Section 1, we have established six coordinate systems and presented the coordinate system transformation using matrix rotation and translation. Quaternions can easily represent vector rotations, they can also realize coordinate translation by means of vector synthesis and decomposition. Figure 1 can be simplified as follows:

In Figure 2, point p is the measuring tip of the system and p' is the point after rotation. P and P' are used to denote their homogeneous coordinates. The

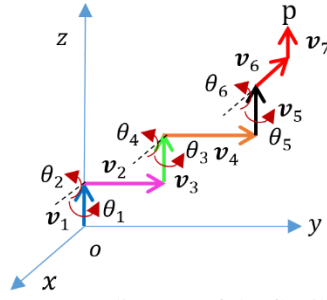


Figure 2: Vector diagram of the flexible CMM

position of the measuring tip in $oxyz$ can be obtained by a series of coordinate transformations and translations. The position vector \overline{op} is composed of seven parts:

$$\overline{op} = \mathbf{v}_1 + \mathbf{v}_2 + \mathbf{v}_3 + \mathbf{v}_4 + \mathbf{v}_5 + \mathbf{v}_6 + \mathbf{v}_7 \quad (17)$$

where \mathbf{v}_6 and \mathbf{v}_7 rotate $\theta_6, \theta_5, \theta_4, \theta_3, \theta_2$ and θ_1 around respective axes which are parallel to ox or oz . Similarly, \mathbf{v}_5 rotates $\theta_5, \theta_4, \theta_3, \theta_2$ and θ_1 ; \mathbf{v}_4 rotates $\theta_4, \theta_3, \theta_2$ and θ_1 ; \mathbf{v}_3 rotates θ_3, θ_2 and θ_1 ; \mathbf{v}_2 rotates θ_2 and θ_1 ; and \mathbf{v}_1 rotates θ_1 around oz . Further, $\mathbf{v}_1 \sim \mathbf{v}_7$ are parallel to coordinate axes, which could simplify the calculation process.

We can define seven coordinate systems based on the above vectors. Then the rotational result $\overline{op'}$ can be obtained by matrix transformations:

$$P' = R_1(R_2(R_3(R_4(R_5(R_6(P + T_6) + T_5) + T_4) + T_3) + T_2) + T_1) \quad (18)$$

where $R_i (4 \times 4)$ and $T_i (4 \times 1) (i = 1, 2, \dots, 6)$ are the rotation matrix and translation matrix.

However, according to (14), the rotation may be represented as:

$$R_i P = Q_i \overline{op} Q_i^* \quad (19)$$

And it is easy to know that T_i is equivalent to \mathbf{v}_i . Hence, (18) could be rewritten as:

$$\overline{op'} = Q_{06}(\mathbf{v}_6 + \mathbf{v}_7)Q_{06}^* + Q_{05}\mathbf{v}_5Q_{05}^* + Q_{04}\mathbf{v}_4Q_{04}^* + Q_{03}\mathbf{v}_3Q_{03}^* + Q_{02}\mathbf{v}_2Q_{02}^* + Q_{01}\mathbf{v}_1Q_{01}^* \quad (20)$$

where $Q_{06} = Q_1 Q_2 Q_3 Q_4 Q_5 Q_6$, $Q_{05} = Q_1 Q_2 Q_3 Q_4 Q_5$, $Q_{04} = Q_1 Q_2 Q_3 Q_4$, $Q_{03} = Q_1 Q_2 Q_3$, $Q_{02} = Q_1 Q_2$ and $Q_{01} = Q_1$; and

$$\begin{cases} Q_1 = \cos \frac{\theta_1}{2} + \mathbf{k} \sin \frac{\theta_1}{2}, Q_3 = \cos \frac{\theta_3}{2} + \mathbf{k} \sin \frac{\theta_3}{2}, Q_5 = \cos \frac{\theta_5}{2} + \mathbf{k} \sin \frac{\theta_5}{2} \\ Q_2 = \cos \frac{\theta_2}{2} + \mathbf{i} \sin \frac{\theta_2}{2}, Q_4 = \cos \frac{\theta_4}{2} + \mathbf{i} \sin \frac{\theta_4}{2}, Q_6 = \cos \frac{\theta_6}{2} + \mathbf{i} \sin \frac{\theta_6}{2} \end{cases} \quad (21)$$

According to (20), the vector $\overrightarrow{op'}$ is decomposed into seven different vectors, which include related rotation information. The result can be obtained by calculating every vector's rotation, and it can be completed in one coordinate system.

3.2 Measurement error analysis

In practical applications, the measurement accuracy of the flexible CMM is seriously affected due to arm length error, misalignment error, nonperpendicularity, initialization error and etc. Assume the rotation angle errors of the six angular encoders are $\Delta\theta_i (i = 1, 2, \dots, 6)$, the joint arm length error are $\Delta d_i (i = 1, 2, \dots, 7)$, the nonperpendicularity errors between the i th and $(i - 1)$ th joint arms $(i = 1, 2, \dots, 7)$ are $\delta_{\alpha i}$ and $\delta_{\beta i}$. When $i = 1$, $\delta_{\alpha 1}$ and $\delta_{\beta 1}$ are the nonperpendicularity errors of the first arm relative to the base. In the ideal measurement model presented in Figure 2, intersection errors are also neglected, we define the intersection errors are Δa_i and $\Delta b_i (i = 1, 2, \dots, 7)$.

3.2.1 Rotation angle errors

Rotation angle error of each rotational joint mainly comes from initialization and reading error. It can be conveniently denoted by encoder readouts and can be easily compensated, e.g. by rotating the same minute angle at relevant joint.

3.3.2 Nonperpendicularity

Ideally, the adjacent flexible arms of CMM are perpendicular to each other at zero positions. However, axis nonperpendicularity may result from the assembling process, with misalignments in each axis. Arm 1 and arm 2, arm 3 and arm 4, arm 5 and arm 6 can be analysed as three respective pairs. Similar to the error analysis of two axial platform, the nonperpendicularity errors could be denoted by minute changes of the rotation angle of each encoder [8]. Take arm 1 and arm 2 for example, direction of v_2 is the initial pointing direction and the errors are presented in Figure 3.

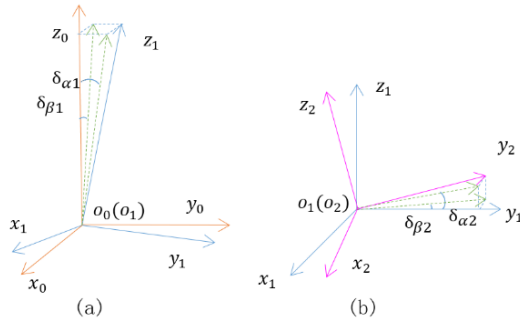


Figure 3: Nonperpendicularity

$o_0x_0y_0z_0$ in Figure 3 is the base's coordinate system, $o_1x_1y_1z_1$ is the first arm's coordinate system, $o_2x_2y_2z_2$ is the second arm's coordinate system. Ideally, the three coordinate systems coincide at zero position. Due to nonperpendicularity, however, $\delta_{\alpha 1}$ and $\delta_{\beta 1}$ are inclined angular components between $o_0x_0y_0z_0$ and $o_1x_1y_1z_1$ along x and y axes, respectively. $\delta_{\alpha 2}$ and $\delta_{\beta 2}$ are inclined angular components between $o_1x_1y_1z_1$ and $o_2x_2y_2z_2$ along x and z axes, respectively. \overrightarrow{op} (parallel to o_0y_0) rotates θ_2 and θ_1 around x and z axes, and the expected pointing direction of $\overrightarrow{op'}$ can be obtained by:

$$\overrightarrow{op'} = (Q_1Q_2)\overrightarrow{op}(Q_1Q_2)^* = i\cos\theta_2\cos\theta_1 + j\sin\theta_2\cos\theta_1 - k\sin\theta_1 \quad (22)$$

Due to the nonperpendicularity errors, the actual pointing error would be biased. Assume $\Delta\theta_{in}(i = 1, 2, \dots, 7)$ as the effect on θ_i , the nonperpendicularity effects due to arms 1 and 2 can be shown in Table 1 [8]:

Table 1: nonperpendicularity effects on encoder readouts

	$\delta_{\alpha 1}$	$\delta_{\beta 1}$	$\delta_{\alpha 2}$	$\delta_{\beta 2}$
$\Delta\theta_{1n}$	$\delta_{\alpha 1}\cos\theta_1\tan\theta_2$	$\delta_{\beta 1}\sin\theta_1\tan\theta_2$	$\delta_{\alpha 2}\tan\theta_2$	$\delta_{\beta 2}$
$\Delta\theta_{2n}$	$-\delta_{\alpha 1}\sin\theta_1$	$\delta_{\beta 1}\cos\theta_1$	0	0

The nonperpendicularity effects due to arms 3 and 4, and arms 5 and 6 could be similarly obtained.

3.3.3 Arm length error

In the ideal measuring model presented in (20), the norm of each vector is the corresponding arm length. The arm length error would affect final position coordinates. For example, $|\mathbf{v}_6|$ is ideal length of the sixth arm, Δd_6 is the length error, the actual length is hence $(|\mathbf{v}_6| + \Delta d_6)$. Assume p'' is the actual final point, according to (20), its effect on the coordinate change can be denoted by:

$$\overrightarrow{p'p''} = Q_{06}\left(\frac{\Delta d_6}{|\mathbf{v}_6|}\mathbf{v}_6\right)Q_{06}^* \quad (23)$$

The effects of the other arm length errors can be obtained in the same way.

3.3.4 Intersection error

The intersection error means two intersecting axes do not exactly intersect. It produces a minute translation along two perpendicular directions, as shown in Figure 4.

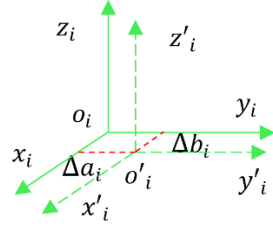


Figure 4: Intersection error

$o_i x_i y_i z_i$ is ideal position, $o'_i x'_i y'_i z'_i$ is actual position, Δa_i and Δb_i are the biases. Take the third arm's intersection error for example, we have:

$$\overline{op} = v_1 + (v_2 + v_{\Delta a_3} + v_{\Delta b_3}) + v_3 + v_4 + v_5 + v_6 + v_7 \quad (24)$$

Then, according to (20), its effect on the coordinate change can be denoted as:

$$\overline{p'p''} = Q_{02}(v_{\Delta a_3} + v_{\Delta b_3})Q_{02}^* \quad (25)$$

The effects of the other intersection errors can be similarly determined.

3.3.4 Error summary

According to the above discussions, rotation angle error and nonperpendicularity can be denoted by encoder readouts, and can be easily compensated by adjusting encoders' inputs. Length error and intersection error on the other hand would cause coordinate's translation, which are better to be compensated by final coordinate transformation. The relevant errors are respectively presented and summarised in Tables 2, 3 and 4.

Table 2: Rotation angle errors denoted by encoder readouts

Encoder readouts	$\Delta\theta_1$	$\Delta\theta_2$	$\Delta\theta_3$	$\Delta\theta_4$	$\Delta\theta_5$	$\Delta\theta_6$
θ_1	$\Delta\theta_1$	0	0	0	0	0
θ_2	0	$\Delta\theta_2$	0	0	0	0
θ_3	0	0	$\Delta\theta_3$	0	0	0
θ_4	0	0	0	$\Delta\theta_4$	0	0
θ_5	0	0	0	0	$\Delta\theta_5$	0
θ_6	0	0	0	0	0	$\Delta\theta_6$

Table 3: Nonperpendicularity errors denoted by encoder readouts

Encoder readouts	$\delta_{\alpha i}$	$\delta_{\beta i}$	$\delta_{\alpha(i+1)}$	$\delta_{\beta(i+1)}$
θ_i	$\delta_{\alpha i} \cos \theta_i \tan \theta_{i+1}$	$\delta_{\beta i} \sin \theta_i \tan \theta_{i+1}$	$\delta_{\alpha(i+1)} \tan \theta_{i+1}$	$\delta_{\beta(i+1)}$
θ_{i+1}	$-\delta_{\alpha i} \sin \theta_i$	$\delta_{\beta i} \cos \theta_i$	0	0

Table 4: Partial error effects on measuring tip position

Arm length errors	$\overline{p'p''}$	Intersection errors	$\overline{p'p''}$
Δd_1	$Q_{01} \left(\frac{\Delta d_1}{ \mathbf{v}_1 } \mathbf{v}_1 \right) Q_{01}^*$	$\Delta a_1, \Delta b_1$	$\mathbf{v}_{\Delta a_1} + \mathbf{v}_{\Delta b_1}$
Δd_2	$Q_{02} \left(\frac{\Delta d_2}{ \mathbf{v}_2 } \mathbf{v}_2 \right) Q_{02}^*$	$\Delta a_2, \Delta b_2$	$Q_{01} (\mathbf{v}_{\Delta a_2} + \mathbf{v}_{\Delta b_2}) Q_{01}^*$
Δd_3	$Q_{03} \left(\frac{\Delta d_3}{ \mathbf{v}_3 } \mathbf{v}_3 \right) Q_{03}^*$	$\Delta a_3, \Delta b_3$	$Q_{02} (\mathbf{v}_{\Delta a_3} + \mathbf{v}_{\Delta b_3}) Q_{02}^*$
Δd_4	$Q_{04} \left(\frac{\Delta d_4}{ \mathbf{v}_4 } \mathbf{v}_4 \right) Q_{04}^*$	$\Delta a_4, \Delta b_4$	$Q_{03} (\mathbf{v}_{\Delta a_4} + \mathbf{v}_{\Delta b_4}) Q_{03}^*$
Δd_5	$Q_{05} \left(\frac{\Delta d_5}{ \mathbf{v}_5 } \mathbf{v}_5 \right) Q_{05}^*$	$\Delta a_5, \Delta b_5$	$Q_{04} (\mathbf{v}_{\Delta a_5} + \mathbf{v}_{\Delta b_5}) Q_{04}^*$
Δd_6	$Q_{06} \left(\frac{\Delta d_6}{ \mathbf{v}_6 } \mathbf{v}_6 \right) Q_{06}^*$	$\Delta a_6, \Delta b_6$	$Q_{05} (\mathbf{v}_{\Delta a_6} + \mathbf{v}_{\Delta b_6}) Q_{05}^*$
Δd_7	$Q_{06} \left(\frac{\Delta d_7}{ \mathbf{v}_7 } \mathbf{v}_7 \right) Q_{06}^*$	$\Delta a_7, \Delta b_7$	$Q_{06} (\mathbf{v}_{\Delta a_7} + \mathbf{v}_{\Delta b_7}) Q_{06}^*$

4 Discussions and conclusions

Denavit-Hartenberg parametric method (D-H method) as a common way of describing the measuring equations and error models of flexible CMMs has been widely used. However, to obtain the measurement model, it is necessary to define six or more coordinate systems, involving complex coordinate system transformations. Quaternions adopted in this paper can describe rotations in a concise way. It only needs to establish a coordinate system for the flexible CMM system, the measurement model is thus easy to obtain through composition of the rotations of vector components, with each parameter having clear physical meaning.

With regard to the error analysis, the flexible CMM system used in this paper contains 39 sources, including rotation angle errors, arm length errors, nonperpendicularity and intersection errors, whilst additional effects due to gravity deformation, temperature and other environment impacts are not considered. The D-H method directly added each error's influence to relevant matrix, and all the results were presented in the position change of the final measuring tip. In this paper, we have analyzed causes of each error, and their

effects can be easily obtained by relevant quaternion rotations. It is also easy to determine each error source's contribution to the total measurement error. Further, for rotation angle error and nonperpendicularity, their effects may be directly denoted by encoders' readout errors, which can be convenient for the subsequent compensation. The rest of the error sources may be represented by final coordinate transformation.

It can be concluded that quaternion method adopted in this paper has a clearer physical meaning, with each error effect clearly presented. As a quaternion has fewer elements than matrix presentation, it would speed up the calculation process and also simplify the modelling process.

References

- [1]X.Y. Wang, S.G. Liu, B. Wang, G.X. Zhang. Mathematical model and error analysis of the articulated arm flexible CMM. *Nanotechnology and Precision Engineering*, 2005,3:262-267.
- [2]B. Karan, M. Vukobratovic. Calibration and accuracy of manipulation robot models-an overview. *Mech. Mach. Theory*, 1994,29:479-500.
- [3]J. Devavit and R. Hartenberg. A kinematic rotation for lower pair mechanism based on matrices. *ASME Journal of Applied Mechanics*, 1955,22:215-221.
- [4]B. Wang, S.G. Liu, X.Y. Wang, G.X. Zhang. Mathematical model and simplifying of parameters of the articulated arm flexible CMM. *Manufacturing Technology & Machine Tool*, 2007,7:52-55.
- [5] L. Meister Mathematical modelling in geodesy based on quaternion algebra *Phys. Chem. Earth (A)*, 2000,25:661-665.
- [6] L. Meister and H. Schaeben. A concise quaternion geometry of rotations *Math. Meth. Appl. Sci.*, 2005, 28:101-126.
- [7] R. Goldman. Understanding quaternions. *Graphical Models*, 2011,73:21-49.
- [8] Q. J. Tang, X.J. Wang, Q. Yang. Static pointing error analysis of electro-optical detection systems. *Proc IMechE, Part B: J Engineering Manufacture*, 2014, DOI:10.1177/0954405414551107.